Nonlin. Processes Geophys. Discuss., doi:10.5194/npg-2016-14, 2016
Manuscript under review for journal Nonlin. Processes Geophys.
Published: 23 February 2016

Nonlinear Processes in Geophysics
Discussions
Open Access
EGU

Multifractal behaviour of the soil water content of a vineyard in NW Spain during two growing seasons

J. M. Mirás-Avalos[1,2], E. Trigo-Córdoba[1], R. da Silva-Dias[3], I. Varela-Vila[3] and A. García-Tomillo[3]

[1]{Estación de Viticultura e Enoloxía de Galicia, EVEGA-INGACAL, Ponte San Clodio s/n, 32428, Leiro, Ourense, Spain}

[2]{Departamento de Riego, Centro de Edafología y Biología Aplicada del Segura, CEBAS-CSIC, Campus Universitario de Espinardo, 31000, Murcia, Spain}

[3]{Área de Edafología y Química Agrícola, Facultad de Ciencias, Universidade da Coruña. Campus A Zapateira s/n 15008 A Coruña, Spain}

Correspondence to: J. M. Mirás-Avalos (jose.manuel.miras.avalos@xunta.es)

Abstract

Soil processes are characterized by a great degree of heterogeneity, which may be assessed by scaling properties. The aims of the current study were to describe the dynamics of soil water content at three depths in a vineyard under rain-fed and irrigation conditions and to assess the multifractality of these time data series. Frequency domain reflectometry (FDR) sensors were used for automatically monitoring soil water content in a vineyard located in Leiro (Ourense, NW Spain). Data were registered at 30-minute intervals at three depths (20, 40 and 60 cm) between 14th June and 26th August 2011 and 2012. Two treatments were considered: rain-fed and irrigation to 50% crop evapotranspiration. Soil water content data series obeyed power laws and tended to behave as multifractals. Values for entropy (D_1) and correlation (D_2) dimensions were lower in the series from the irrigation treatment. The Hölder exponent of order zero (α_0) was similar between treatments; however, the widths of the singularity spectra, $f(\alpha)$, were greater under irrigation conditions. Multifractality indices slightly decreased with depth. These results suggest that singularity and Rényi spectra were useful for characterizing the time variability of soil water content, distinguishing patterns among series registered under rain-fed and irrigation treatments.

Nonlin. Processes Geophys. Discuss., doi:10.5194/npg-2016-14, 2016
Manuscript under review for journal Nonlin. Processes Geophys.
Published: 23 February 2016

Nonlinear Processes in Geophysics
Discussions
Open Access
EGU

1 Introduction

Soil water storage variability is strongly related with topographical, geological, edaphic and vegetation factors (Braud et al., 1995). These environmental factors and processes (rainfall, evapotranspiration, runoff) do not operate independently but as a conjunction of processes with nested and complex effects. Overall, this results in a distribution of soil water storage that varies as a function of the temporal and spatial scales. Therefore, similar to other soil properties and processes (Western and Blöschl, 1999; Zeleke and Si, 2006), soil water storage along time is a complex process characterized by a lack of homogeneity; heterogeneity in space and/or time is a feature that can be described by scaling procedures.

Fractals have been widely employed in soil science, as soil properties may be described through scale invariance concepts (Tyler and Wheatcraft, 1990; Perfect et al., 1996; Vidal Vázquez et al., 2007; Biswas et al., 2012a). More recently, several authors performed multifractal studies of heterogeneous time data series. For instance, Jiménez-Hornero et al. (2010) described ozone time series using the multifractal formalism. Rodríguez-Gómez et al. (2013) used a multifractal approach for characterizing solar radiation time series.

Soil water content can be automatically estimated by using sensors that measure variations in the soil dielectric constant, since it is strongly related with soil water content (Mestas-Valero et al., 2012). This parameter is characterized by its spiky dynamics, with sudden and intense peaks of high frequency activity, mostly at soil surface. Several studies have described scaling patterns for the behaviour of sol water content spatial distribution (e.g. Kim and Barros, 2002; Biswas et al., 2012b); however, multifractal analyses of continuously measured soil water content are scarce, except for a study on rain-fed grassland (Mestas-Valero et al., 2011). Therefore, the aim of the current work was to describe soil water dynamics in a vineyard subjected to two different treatments (rain-fed and irrigated) and to assess multifractality of these data series over two consecutive seasons.

Nonlin. Processes Geophys. Discuss., doi:10.5194/npg-2016-14, 2016
Manuscript under review for journal Nonlin. Processes Geophys.
Published: 23 February 2016

2 Materials and Methods

2.1 Description of the study area

The experiment was conducted over two consecutive growing seasons (2011-2012) in a 0.2-ha vineyard (*Vitis vinifera* L.) planted with cultivar 'Albariño', located in the experimental farm of the Estación de Viticultura e Enoloxía de Galicia (EVEGA), in Leiro (42º 21.6' N, 8º 7.02' W, elevation 115 m), Ourense, Spain (Fig. 1). Vines were grafted in 1998 on 196-17C rootstock and trained to a vertical trellis on a single cordon system (10-12 buds per vine). Rows were east-west oriented, spacings between vines and between rows were 1.25 and 2.4 m, respectively (3333 vines ha^{-1}). The soil at the site was sandy-textured (64% sand, 16% silt, 20% clay), slightly acidic (pH 6.3), medium fertility (2.7% organic matter) and with a rather shallow profile (≈1.2 m). The climate of the studied site is temperate, humid with cool nights (Fraga et al., 2014).

2.2 Experimental design

The reference evapotranspiration (ET_0) per week for the site was calculated from weather variables recorded at a station located 150 m away from the experimental vineyard using the Penman-Monteith equation (Allen et al., 1998). The ET_0 was then used, along with a constant crop coefficient (K_c = 0.8) to compute the amount of water required by the vines (Trigo-Córdoba et al., 2015). Precipitation was substracted from ET_c each week. The calculated amount of water was applied the following week.

Treatments consisted of a rain-fed control and an irrigation to the 50% of ET_c. Irrigation was applied from late June (after bloom) till mid-August, approximately two weeks prior to harvest through two pressure-compensated emitters of 4 L h^{-1} located 25 cm on either side of the vine. Irrigation water was of good quality, with pH of 6.35, electrical conductivity of 163.4 µS cm^{-1} and 0.4 mg of suspended solids. The water amount applied each season was 40 and 50 mm for 2011 and 2012, respectively (Table 1).

2.3 Measurements

The volumetric soil water content was continuously monitored through the soil profile in two spots of the experimental vineyard (one in the rain-fed treatment and another in the irrigated treatment) using two capacitance probes (EnviroSCAN, Sentek, Australia), based on the

Nonlin. Processes Geophys. Discuss., doi:10.5194/npg-2016-14, 2016
Manuscript under review for journal Nonlin. Processes Geophys.
Published: 23 February 2016

frequency domain reflectometry (FDR) technique. Each probe was equipped with three sensors installed on an access tube at 20, 40 and 60 cm depth and connected to a datalogger. The probes were properly maintained for recording soil water content at half-hour intervals over the 2011 and 2012 seasons. Here, data from the irrigation period (mid-June to late-August) are reported.

In each treatment, the probe was located within two vines (Fig. 1), avoiding to be close to the emitters (25 cm from the emitter and 50 cm from the vine trunk, approximately). The equation provided by the manufacturer was used for transforming permitivity data registered by the probes into soil water content.

2.4 Multifractal analysis

The concepts of multifractals and their estimation methods that were used in the current study are next summarized. For detailed descriptions about multifractals, further information can be found in Chhabra et al. (1989) and Everstz and Mandelbrot (1992).

To implement the multifractal analysis of one-dimensional soil water content time distributions supported on a given interval I = [a, b], a set of not-overlapping sub-intervals of I with equal length is required. A common choice is to consider dyadic scaling down (Everstz and Mandelbrot, 1992; Caniego et al., 2005), which means successive partitions of I in k stages (k = 1, 2, 3…). Hence, at each scale, d, a number of segments, $N(\delta) = 2^k$ are obtained with characteristic time resolution, $\delta = L \times 2^{-k}$, covering the whole extent of I.

Multifractal approach applied to time series has already been described (Jiménez-Hornero et al., 2010), hence, we only summarize the technique used in the current study. The time interval of soil water content data series, L, varied from half an hour to two months and the minimum time resolution, δ_{ini}, was chosen accounting for containing at least one half-hourly averaged soil moisture data, θ_{ini}, at every initial interval. According to this, the probability mass distribution, $p_i(\delta)$, at time resolution δ was estimated as:

$$p_i(\delta) = \frac{\theta_i(\delta)}{\sum_{j}^{n_{ini}} (\theta_{ini})_j} \quad (1)$$

where θ_i is the water content of the i^{th} interval and n_{ini} is the number of initial intervals with mean soil water content θ_{ini}.

Nonlin. Processes Geophys. Discuss., doi:10.5194/npg-2016-14, 2016
Manuscript under review for journal Nonlin. Processes Geophys.
Published: 23 February 2016

The method of the moments was used (Chhabra et al., 1989) to analyze the multifractal spectrum of the probability mass function, $p_i(\delta)$. The partition function $\chi(q, \delta)$ was estimated:

$$\chi(q,\delta) = \sum_{i=1}^{n} p_i(\delta)^q \qquad (2)$$

were moment q is a real number between -∞ and +∞.

A log-log plot of the partition function versus δ for different values of q yields:

$$\chi(q,\delta) \propto \delta^{-\tau(q)} \qquad (3)$$

were $\tau(q)$ is the mass scaling function of order q. The functions $f(\alpha)$ and α can be obtained by Legendre transformation of the mass exponent, $\tau(q)$, as: $f(\alpha) = \alpha(q) - \tau(q)$ and $\alpha(q) = d\tau(q)/dq$, respectively. Log-log plots of $\chi_q(\delta)$, versus δ, however, typically exhibit linearity across a limited scale range (e.g. Posadas et al., 2003), which results in drawbacks when using the moment method to obtain the singularity spectrum.

The direct method (Chhabra and Jensen, 1989) avoid inaccuracies associated to the estimation of $\alpha(q)$ by Legendre transformation. This method is based on the calculation of the contributions of individual segments, $\mu_i(q,\delta)$, to the partition function, which are defined as:

$$\mu_i(q,\delta) = \mu_i^{\,q}(\delta) / \sum_1^{N(\delta)} \mu_i^{\,q}(\delta) \qquad (4)$$

Then, using a set of real numbers, q, ($-\infty < q < -\infty$), the relationships applied to calculate $f(\alpha)$ and α, can be expressed as:

$$f(\alpha(q)) \propto \frac{\sum_{i=1}^{N(\delta)} \mu_i(q,\delta) \log[\mu_i(q,\delta)]}{\log(\delta)} \qquad (5a)$$

and

$$\alpha(q) \propto \frac{\sum_{i=1}^{N(\delta)} \mu_i(q,\delta) \log[\mu_i(\delta)]}{\log(\delta)} \qquad (5b)$$

The $f(\alpha)$–α spectrum is reduced to a point for monofractal scaling type. The minimum scaling exponent (α_{min}) corresponds to the most concentrated region of the measure, and the maximum exponent (α_{max}) corresponds to the rarefied regions of the measure. A plot of $f(\alpha)$ vs. α is called multifractal spectrum. It is a downward function with a maximum at $q = 0$. The width of the multifractal spectrum ($w = \alpha_{max} - \alpha_{min}$) indicates overall variability (Moreno et al., 2008) similar to the nugget effects in geostatistics. For each data series, we calculated

Nonlin. Processes Geophys. Discuss., doi:10.5194/npg-2016-14, 2016
Manuscript under review for journal Nonlin. Processes Geophys.
Published: 23 February 2016

multifractal spectrum with q from –10 to +10 in steps of 0.5, fine enough to show the multifractal behaviour in the studied moment range.

Multifractal measures can also be characterized on the basis of the generalized dimension, D_q, of the moment of order q of a distribution, defined by Grassberger and Procaccioa (1983), based on the work of Rényi (1955). The D_q, of a multifractal measure is calculated as:

$$D_q = \frac{\tau(q)}{q-1} = \frac{1}{q-1}\lim_{\delta\to 0}\frac{\log\left[\chi_q(\delta)\right]}{\log\delta}\ ,\ q\neq 1 \qquad (6a)$$

and

$$D_1 \approx \lim_{\delta\to 0}\frac{\sum_{i=1}^{n(\delta)}\mu_i(\delta)\log\left[\mu_i(\delta)\right]}{\log\delta},\ q=1 \qquad (6b)$$

Equation (6a) shows that $\tau(q)$ is also related to the generalized fractal dimension, D_q. In fact, the concept of generalized dimension, D_q, corresponds to the scaling exponent for the q^{th} moment of the measure. Using equation (6a), D_1 becomes indeterminate. Therefore, for the particular case that q =1, equation (6b) was employed.

For a monofractal, D_q is a constant function of q. However, for multifractal measures, the relationship between D_q and q is described by a S-shaped curve. In this case, the most frequently used generalized dimensions are D_0 for q = 0, D_1 for q = 1 and D_2 for q = 2, which are referred to as capacity, information (or Shannon entropy) and correlation dimension, respectively. The information dimension, D_1, provides insight about the degree of heterogeneity in the distribution of the measure. The correlation dimension, D_2, is associated to the uniformity of the measure among intervals and describes the average distribution density of the measure. In general, the generalized dimension, D_q, is more useful for the comprehensive study of multifractals. Differences between D_q allow comparison of the complexity between measured soil water content data series. In homogeneous structures D_q are close, whereas in a monofractal they are equal.

Nonlin. Processes Geophys. Discuss., doi:10.5194/npg-2016-14, 2016
Manuscript under review for journal Nonlin. Processes Geophys.
Published: 23 February 2016

3 Results and discussion

3.1 Patterns of vineyard soil water content under rain-fed and irrigation conditions

Temperatures for the two studied growing seasons were similar in average (Table 1); however, rainfall and evapotranspiration were higher in 2012. Harvest date was almost the same in both years. Nevertheless, the temporal evolution of rainfall and ET_c differed from year to year (Fig. 2), being greater during 2012, especially at the beginning of the study period. This fact caused a different scheduling of irrigation between years.

Soil water content decreased over the growing season under rain-fed conditions in both years (Fig. 3). However, when irrigation was initiated, soil water content became more stable in the irrigated treatment (Fig. 3). The magnitude of the soil water loss was more evident in the layers of 20 and 40 cm depth, and less important in the 60 cm layer, which may indicate the depth of the active root zone as well as the intensity of root water uptake at each soil layer, as reported for other cultivars and crops (Intrigliolo and Castel, 2009; Mestas-Valero et al., 2011), and proved that FDR probes can be successfully used for irrigation scheduling (Goldhamer et al., 1999), calibrating them with established indicators such as midday stem water potential (Mirás-Avalos et al., 2014). Indeed, our results suggest that the water amount applied through irrigation was enough for fulfilling vineyard water requirements over the two growing seasons studied.

3.2 Multifractality of the soil water content time series

Soil water content time series obeyed power law scaling, as shown by the double log plots (Fig. 4). These plots allow to identify the range of moments needed to describe the scale variation of the studied parameter (Vidal Vázquez et al., 2010).

Figure 4 shows the partition functions for rain-fed and irrigation conditions at 20 cm depth in 2011. Visually, a slight departure from the straight line model was observed for moments $q < -1$ (Fig. 4). In general, higher deviations from linearity were found for the highest q moments in the data series from the irrigation treatment, when compared to those from the rain-fed treatment, especially in 2012. Nevertheless, determination coefficients, R^2, were greater than 0.9 for statistical moments in the range from $q = -10$ to $q = 10$, in all the studied data sets.

Nonlin. Processes Geophys. Discuss., doi:10.5194/npg-2016-14, 2016
Manuscript under review for journal Nonlin. Processes Geophys.
Published: 23 February 2016

Consequently, scalings are adequately defined. Similar results were found by Mestas-Valero et al. (2011) for soil water content under rain-fed grassland.

The $\tau(q)$ functions were different from a monofractal type of scaling for all series analyzed, especially under irrigation conditions (Fig. 5), similar to results obtained by Biswas et al. (2012b) for soil water storage. In fact, the hetereogeneity of the soil water content data series from the irrigated treatment was greater than that of the rain-fed treatment (Fig. 5).

The value of D_1 is a good indicator of the heterogeneity degree in temporal distributions of a given variable. The closer the D_1 value to D_0, the more homogeneous is the distribution of the variable. In our case, rain-fed series were more homogeneous than the irrigated ones. In general, soil water content recorded at 60 cm depth presented the lower differences between D_1 and D_0 (Table 2), thus being more homogeneous both under rain-fed and irrigation conditions. Moreover, 2012 data series presented a higher hetereogeneity than those from 2011 (Table 2) for both treatments, caused by the greater rainfall amount collected in 2012.

A monofractal would be characterized by $D_0 = D_1 = D_2$ (Evertsz and Mandelbrot, 1992). In all the studied data series $D_0 > D_1 > D_2$ (Table 2), indicating that soil water content had a tendency to behave as a multifractal. However, differences ($D_0 - D_1$) ranged from 0.051 to 0.222 and ($D_1 - D_2$) oscillated between 0.053 and 0.168, which suggests different degree in the homogeneity/heterogeneity of soil water content depending on the treatment imposed and the depth in the soil profile. In general, data series from the irrigation treatment showed greater differences between D_0, D_1 and D_2 than the series from the rain-fed treatment for both growing seasons. Moreover, the 60 cm depth layer presented smaller differences than the 20 and 40 cm layers (Table 2). The width of the D_q spectra, determined by indicators such as ($D_0 - D_{10}$), showed different degrees of hetereogeneity, with a trend to decrease in depth and under rain-fed conditions when compared with the irrigation treatment (Table 2). This is caused by the spiky nature of soil water content and indicates a multiple scaling nature at shallow depths.

Generalized dimensions, or Rényi spectra, calculated for the range between q = -10 and q = 10 for soil water content data series at three depths under rain-fed and irrigation conditions are displayed on Fig. 6. All the data series studied showed Rényi spectra as asymmetric sigma-shaped curves with more curvature for the negative values of q than for positive ones (Fig. 6). The left part of the curves is concave down and it changes to concave up on the right of the vertical axis. In the case of the soil water content series from the rain-fed treatment, the

Nonlin. Processes Geophys. Discuss., doi:10.5194/npg-2016-14, 2016
Manuscript under review for journal Nonlin. Processes Geophys.
Published: 23 February 2016

most curved spectra corresponded to the 40 cm depth data series, whereas for the irrigation treatment, the most curved one was the 20 cm depth data series (Fig. 6). When compared between treatments, Rényi spectra were more curved under irrigation conditions and the estimation errors were also greater under this treatment (Fig. 6). These results confirmed the higher hetereogeneity (multifractality) of the data series from the irrigation treatment when compared to those from rain-fed.

Mestas-Valero et al. (2011) obtained monofractal distributions of soil water content time series under grassland when measured at depths greater than 40 cm, in contrast with our results. This disagreement is likely caused by the fact that grapevine root system reach greater depths than that of grass and vines are capable of uptaking water from deeper soil layers.

Determination coefficients, R^2, were highest for moments $q = 0$ and $q = 1$ and diminished for the other $|q|$ moments. In the case of $q = 10$, R^2 was greater than 0.97 and 0.95 in the rain-fed and irrigated data sets, respectively. For $q = -10$, R^2 values for rain-fed and irrigated data series were greater than 0.99 and 0.91, respectively (data not shown). Standard errors of D_q values increased with increasing $|q|$ moments and they were much lower for right ($q > 0$) than for left ($q < 0$) branch of the Rényi spectra (Fig. 6).

Parameter α_0 from the singularity spectra ranged from 1.056 to 1.146 in the rain-fed treatment and from 1.075 to 1.187 in the irrigated treatment (Table 3). The singularity spectrum allows for analyzing similarity or difference between the scaling properties of the measures as well as to assess the local scaling properties of soil water content measurements. The wider the spectrum is (i.e., the largest $\alpha_{q-} - \alpha_{q+}$ value), the higher the heterogeneity in the scaling indices and vice versa (Vidal Vázquez et al., 2010). Moreover, the $f(\alpha)$ spectrum branch length gives insight about the abundance of the measure. Hence, small $f(\alpha)$ values at the end of a long branch correspond to rare events.

Singularity spectra are characterized by a concave down shape (Fig. 7), showing an asymmetrical curve with wider but shorter right side. Rain-fed data series showed a shorter $f(\alpha)$ spectrum in both years, confirming their low degree of multifractality when compared to the irrigated data series (Fig. 7).

Differences ($\alpha_{q-} - \alpha_0$ and $\alpha_0 - \alpha_{q+}$) indicate the deviation of the spectrum from its maximum value ($q = 0$) towards the right side ($q < 0$) and the left side ($q > 0$), respectively (Vidal Vázquez et al., 2010). Usually, soil water content data series from the rain-fed treatment

Nonlin. Processes Geophys. Discuss., doi:10.5194/npg-2016-14, 2016
Manuscript under review for journal Nonlin. Processes Geophys.
Published: 23 February 2016

showed lower $\alpha_0 - \alpha_{q+}$ values than those from the irrigated treatment (Table 3). Moreover, the highest values for this multifractal parameter were observed at 40 cm depth in both treatments and years (Table 3). This may indicate that higher soil water contents were more frequent under irrigation, being greater the differences between treatments at 40 cm depth in 2012. In contrast, the right branch ($\alpha_{q-} - \alpha_0$) of the spectrum was usually wider for rain-fed conditions (Table 3). These results confirm the differential homogeneity/heterogeneity pattern between treatments evidenced by the generalized dimension, D_q, analysis (Table 2, Fig. 6).

4 Conclusions

Under the conditions of this study, continuous soil water content measurements at different depths reliable described the soil water balance in a vineyard over two irrigation periods.

The logarithms of the partition function varied linearly with the logarithms of the time resolution for all the studied depths under both treatments considered in the range of moments $-10 < q < 10$, indicating that soil water content time series obeyed power laws.

The scaling properties of soil water content time series were reasonably fitted to multifractal models. These properties were different for the rain-fed and irrigation treatments, implying a higher heterogeneity for the data series from the irrigation treatment. Therefore, multifractal analysis allowed us to discriminate among soil water content patterns in a vineyard for the 2011 and 2012 growing seasons as a function of irrigation use.

Author contribution

J. M. Mirás-Avalos and E. Trigo-Córdoba designed and carried out the field experiment. J. M. Mirás-Avalos, R. da Silva-Dias, I. Varela-Vila and A. García-Tomillo performed the analyses. J. M. Mirás-Avalos prepared the manuscript with contributions from all co-authors.

Acknowledgements

This work has been partialy supported by INIA (RTA2011-00041-C02-01), with 80% FEDER funds. J.M. Mirás-Avalos thanks Xunta de Galicia for his ‘Isidro Parga Pondal’ contract. E. Trigo-Córdoba thanks INIA for his FPI scholarship. The authors thank Dr. A Paz González for support and discussion about multifractal analysis.

Nonlin. Processes Geophys. Discuss., doi:10.5194/npg-2016-14, 2016
Manuscript under review for journal Nonlin. Processes Geophys.
Published: 23 February 2016

References

Allen, R. G., Pereira, L. S., Raes, D., and Smith, M.: Crop evapotranspiration. Guidelines for computing crop water requirements, FAO Irrigation and Drainage paper No 56, Rome, Italy, 1998.

Biswas, A., Cresswell, H. P., and Si, B. C.: Application of multifractal and joint multifractal analysis in examining soil spatial variation: A review, Fractal Analysis and Chaos in Geosciences, Dr. Sid-Ali Ouadfeul (Ed.), ISBN: 978-953-51-0729-3, InTech. 2012a.

Biswas, A., Zeleke, T. B., and Si, B. C.: Multifractal detrended fluctuation analysis in examining scaling properties of the spatial patterns of soil water storage, Nonlin. Processes Geophys., 19, 227-238, 2012b.

Braud, I., Dantasantonino, A. C., and Vauclin, M.: Approach to studying the influence of the spatial variability of soil hydraulic properties on surface fluxes, temperature and humidity, J. Hydrol., 165, 283-310, 1995.

Caniego, F. J., Espejo, R., Martín, M. A., and San José, F.: Multifractal scaling of soil spatial variability, Ecol. Model., 182, 291-303, 2005.

Chhabra, A. B. and Jensen, R. V.: Direct determination of the $f(\alpha)$ singularity spectrum, Phys. Rev. Lett., 62, 1327-1330, 1989.

Chhabra, A. B., Meneveau, C., Jensen, R. V., and Sreenivassen, K. R.: Direct determination of the $f(\alpha)$ singularity spectrum and its application to fully developed turbulence, Phys. Rev. A, 40, 5284-5294, 1989.

Everstz, C. J. G. and Mandelbrot, B. B.: Multifractal measures, in Chaos and Fractals, Springer, Berlin, 1992.

Fraga, H., Malheiro, A. C., Moutinho-Pereira, J., Cardoso, R. M., Soares, P. M. M., Cancela, J. J., Pinto, J. G., and Santos, J. A.: Integrated analysis of climate, soil, topography and vegetative growth in Iberian viticultural regions, PLOS One, 9(9), e108078, 2014.

Goldhamer, D. A., Fereres, E., Mata, M., Girona, J., and Cohen, M.: Sensitivity of continuous and discrete plant and soil water status monitoring in peach trees subjected to deficit irrigation, J. Amer. Soc. Hortic. Sci., 124, 437-444, 1999.

Grassberger, P. and Procaccia, I.: Characterization of strange attractors, Phys. Rev. Lett., 50, 346-349, 1983.

Halsey, T. C., Jensen, M. H., Kanadoff, L. P., Procaccia, I., and Shraiman, B.I.: Fractal measures and their singularities: The characterization of strange sets, Phys. Rev. A, 33, 1141-1151, 1986.

Intrigliolo, D. S. and Castel, J. R.: Response of Vitis vinifera cv. 'Tempranillo' to partial rootzone drying in the field: Water relations, growth, yield and fruit and wine quality, Agric. Water Manage., 96, 282-292, 2009.

Jiménez-Hornero, F. J., Gutiérrez de Ravé, E., Ariza-Villaverde, A. B., and Giráldez, J. V.: Description of the seasonal pattern in ozone concentration time series by using the strange attractor multifractal formalism, Environ. Monitor. Assess., 160, 229-236, 2010.

Kim, G. and Barros, A.P.: Space-time characterization of soil moisture from pasive microwave remotely sensed imagery and ancillary data, Remote Sens. Environ., 81, 393-403, 2002.

Korvin, G.: Fractal models in the Earth Sciences, Elsevier, Amsterdam, 1992.

Mestas-Valero, R. M., Valcárcel Armesto, M., Mirás-Avalos, J. M., Vidal Vázquez, E., Paz Ferreiro, J., and Guimarães Giácomo, R.: Temporal trends of water content under grassland: characterization using the multifractal approach, Estudios de la Zona No Saturada del Suelo vol. X, Universidad de Salamanca, 109-112, 2011.

Mestas-Valero, R. M., Mirás-Avalos, J. M., and Vidal Vázquez, E.: Estimation of the daily water consumption by maize under Atlantic climatic conditions (A Coruña, NW Spain) using Frequency Domain Reflectometry, Nat. Hazards Earth Syst. Sci., 12, 709-714, 2012.

Mirás-Avalos, J. M., Trigo-Córdoba, E., and Bouzas-Cid, Y.: Does predawn water potential discern between irrigation treatments in Galician white grapevine cultivars?, J. Int. Sci. Vigne Vin, 48(2), 123-127.

Moreno, R., Díaz Álvarez, M. C., Tarquis Alfonso, A. M., Barrington, S., and Saa Requejo, A.: Tillage and soil type effects on soil surface roughness at semiarid climatic conditions, Soil Till. Res., 98, 35-44, 2008.

Perfect, E., McLaughlin, N. B., Kay, B. D., and Topp, G. C.: An improved fractal equation for the soil water retention curve, Water Resour. Res., 32, 281-287, 1996.

Posadas, A., Jiménez, D., and Quiroz, R.: Análisis multifractal de la variabilidad espacial de la coductividad hidráulica en un suelo estratificado, Rev. Inv. Física, 5, 36-43, 2002.

Posadas, A. N. D., Gimenez, D., Quiroz, R., and Protz, R. Multifractal characterization of soil pore systems, Soil Sci. Soc. Am. J., 67, 1361–1369, 2003.

Rényi, A.: On new axiomatic theory of probability, Acta Math. Hung., 6, 285-335,1955.

Rodríguez-Gómez, B. A., Meizoso-López, M. C., Mirás-Avalos, J. M., García-Tomillo, A., and Paz-González, A.: Assessment of solar irradiation models in A Coruña by multifractal analysis, Vadose Zone J., 12(3), doi:10.2136/vzj2012.0183, 2013.

Trigo-Córdoba, E., Bouzas-Cid, Y., Orriols-Fernández, I., and Mirás-Avalos, J. M.: Effects of deficit irrigation on the performance of grapevine (*Vitis vinifera* L.) cv. 'Godello' and 'Treixadura' in Ribeiro, NW Spain. Agric. Water Manage., 161, 20-30, 2015.

Tyler, W. T. and Wheatcraft, S.: Fractal processes in soil water retention, Water Resour. Res., 26, 1047-1054, 1990.

Vidal Vázquez, E., Miranda, J. G. V., and Paz González, A.: Describing soil surface microrelief by crossover length and fractal dimension, Nonlin. Processes Geophys., 14, 223-235, 2007.

Vidal Vázquez, E., Miranda, J. G. V., and Paz Ferreiro, J.: A multifractal approach to characteriza cumulative rainfall and tillage effects on soil surface micro-topography and to predict depression storage, Biogeosci., 7, 2989-3004, 2010.

Western, A. W. and Blöschl, G.: On spatial scaling of soil moisture, J. Hydrol., 217, 203-224, 1999.

Zeleke, T. B. and Si, B. C.: Characterizing scale-dependent spatial relationships between soil properties using multifractal techniques, Geoderma, 134, 440-452, 2006.

Nonlin. Processes Geophys. Discuss., doi:10.5194/npg-2016-14, 2016
Manuscript under review for journal Nonlin. Processes Geophys.
Published: 23 February 2016

Nonlinear Processes in Geophysics
Discussions
Open Access
EGU

Table 1. Summary of climate variables (temperature, rainfall and ET_0), irrigation water applied and harvest date for the studied period in 2011 and 2012 (from 14th June to 26 August).

Year	Temperature (ºC)			Rainfall	ET_0	Irrigation	Harvest date
	Minimum	Maximum	Average	(mm)	(mm)	(mm)	
2011	12.44	28.86	20.15	25.60	230.78	39.67	14th September
2012	12.33	28.21	19.67	65.60	344.91	50.00	13th September

Nonlin. Processes Geophys. Discuss., doi:10.5194/npg-2016-14, 2016
Manuscript under review for journal Nonlin. Processes Geophys.
Published: 23 February 2016

Table 2. Selected multifractal parameters: generalized dimensions, for the first-three positive moments, D_0, D_1, and D_2, with their respective errors of estimation, and two multifractality indices $\Delta(D_0 - D_2)$ and $\Delta(D_0 - D_{10})$.

Treatment	Depth (cm)	D_0	D_1	D_2	$\Delta(D_0 - D_2)$	$\Delta(D_0 - D_{10})$
			2011			
Rain-fed	20	0.999 ± 0.001	0.937 ± 0.008	0.884 ± 0.016	0.115	0.672
	40	1.000 ± 0.000	0.881 ± 0.007	0.746 ± 0.014	0.254	0.752
	60	1.000 ± 0.000	0.925 ± 0.007	0.868 ± 0.013	0.133	0.656
	20-60	1.000 ± 0.000	0.916 ± 0.008	0.833 ± 0.019	0.167	0.589
Irrigated	20	0.999 ± 0.001	0.868 ± 0.013	0.778 ± 0.026	0.221	0.757
	40	1.000 ± 0.000	0.852 ± 0.019	0.773 ± 0.026	0.227	0.698
	60	1.000 ± 0.000	0.852 ± 0.022	0.758 ± 0.034	0.242	0.664
	20-60	1.000 ± 0.000	0.861 ± 0.023	0.773 ± 0.037	0.227	0.695
			2012			
Rain-fed	20	0.999 ± 0.001	0.861 ± 0.014	0.771 ± 0.025	0.228	0.856
	40	1.000 ± 0.000	0.888 ± 0.008	0.739 ± 0.017	0.261	0.801
	60	1.000 ± 0.000	0.949 ± 0.004	0.907 ± 0.005	0.093	0.548
	20-60	1.000 ± 0.000	0.898 ± 0.006	0.768 ± 0.016	0.232	0.682
Irrigated	20	0.984 ± 0.006	0.831 ± 0.010	0.731 ± 0.019	0.253	1.024
	40	0.979 ± 0.006	0.757 ± 0.014	0.589 ± 0.022	0.390	1.210
	60	1.000 ± 0.000	0.907 ± 0.007	0.805 ± 0.015	0.195	0.622
	20-60	0.993 ± 0.003	0.822 ± 0.016	0.707 ± 0.030	0.286	1.085

Nonlin. Processes Geophys. Discuss., doi:10.5194/npg-2016-14, 2016
Manuscript under review for journal Nonlin. Processes Geophys.
Published: 23 February 2016

Table 3. Selected multifractal parameters derived from the $f(\alpha)$ singularity spectra: most positive (q_+) and most negative (q_-) limits the range of multifractal scaling, Hölder exponent of order 0 (α_0), most positive (α_{q+}) and most negative (α_{q-}) exponents, widths of the let ($\alpha_0 - \alpha_{q+}$) and the right ($\alpha_{q-} - \alpha_0$) sides of the spectra.

Treatment	Depth (cm)	q_-	q_+	α_0	α_{q+}	α_{q-}	$\alpha_0 - \alpha_{q+}$	$\alpha_{q-} - \alpha_0$
				2011				
Rain-fed	20	-1.5	3.5	1.066	0.768	1.339	0.299	0.273
	40	-3.5	2	1.093	0.632	1.328	0.460	0.235
	60	-3.5	2	1.087	0.718	1.403	0.369	0.315
	20-60	-4	2	1.074	0.762	1.297	0.312	0.222
Irrigated	20	-2.5	2	1.136	0.714	1.450	0.422	0.314
	40	-4	3	1.160	0.664	1.383	0.496	0.222
	60	-5	2	1.132	0.700	1.333	0.435	0.200
	20-60	-4.5	2	1.142	0.709	1.375	0.433	0.233
				2012				
Rain-fed	20	-2.5	3	1.146	0.659	1.526	0.487	0.380
	40	-3.5	2	1.082	0.603	1.301	0.479	0.219
	60	-2	5.5	1.056	0.746	1.296	0.309	0.240
	20-60	-5	2	1.077	0.651	1.265	0.426	0.188
Irrigated	20	-0.5	2.5	1.164	0.602	1.361	0.562	0.197
	40	-1	1.5	1.187	0.575	1.491	0.611	0.304
	60	-4	2	1.075	0.716	1.223	0.360	0.148
	20-60	-1	2	1.172	0.624	1.489	0.548	0.317

Nonlin. Processes Geophys. Discuss., doi:10.5194/npg-2016-14, 2016
Manuscript under review for journal Nonlin. Processes Geophys.
Published: 23 February 2016

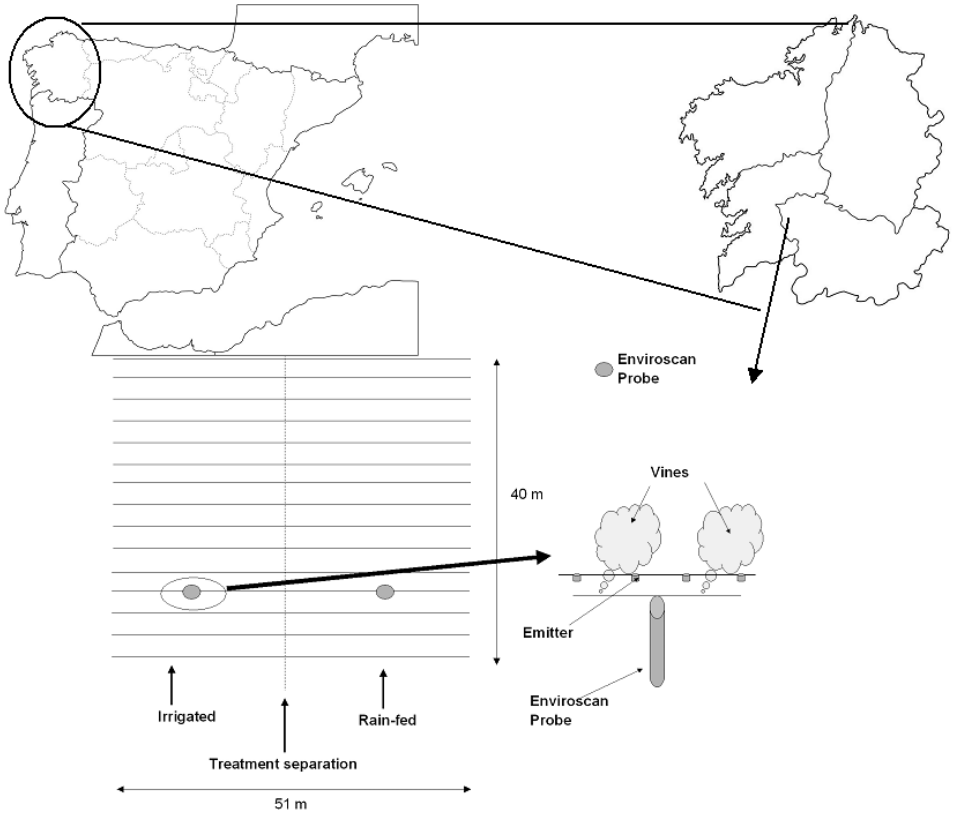

Figure 1. Location of the studied vineyard and experimental layout.

Nonlin. Processes Geophys. Discuss., doi:10.5194/npg-2016-14, 2016
Manuscript under review for journal Nonlin. Processes Geophys.
Published: 23 February 2016

Nonlinear Processes in Geophysics
Discussions
Open Access
EGU

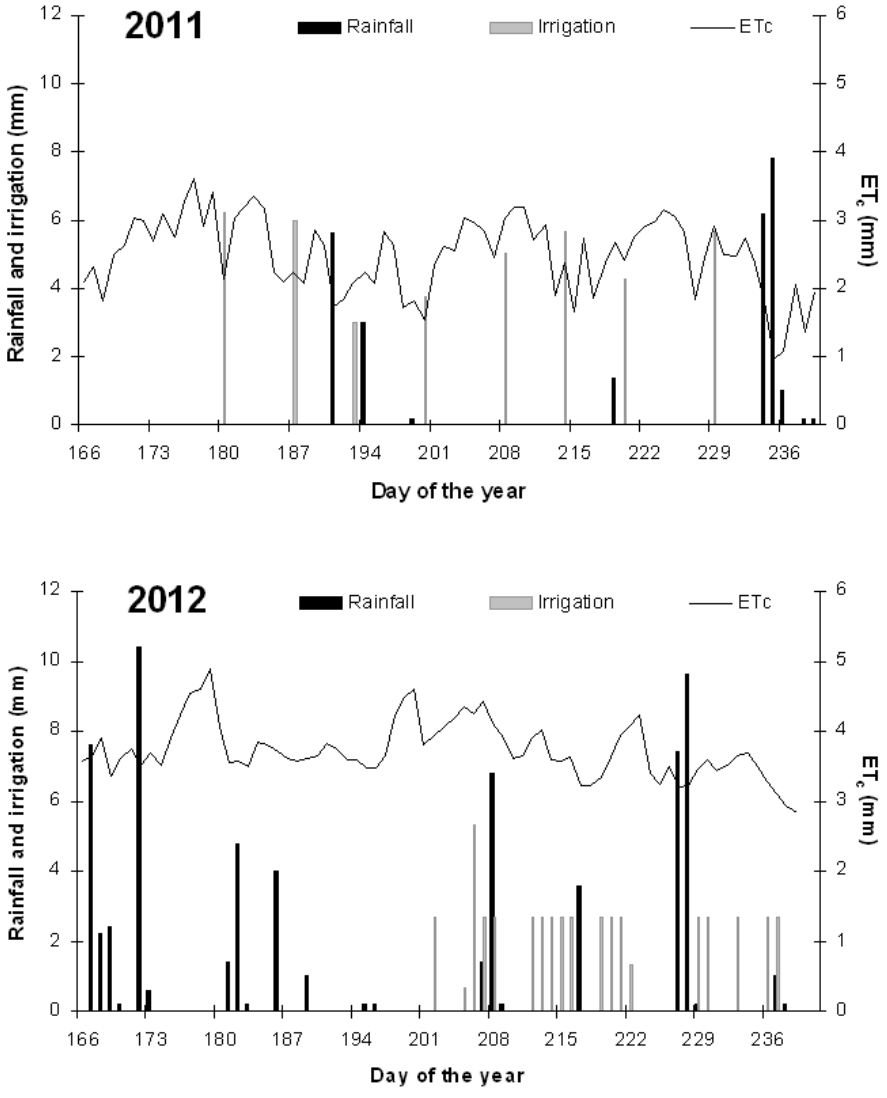

1

2

3 Figure 2. Crop evapotranspiration (ET_c), rainfall and irrigation water applied over the two
4 growing seasons studied, 2011 and 2012. Day of the year 166 is 14th June.

5

Nonlin. Processes Geophys. Discuss., doi:10.5194/npg-2016-14, 2016
Manuscript under review for journal Nonlin. Processes Geophys.
Published: 23 February 2016

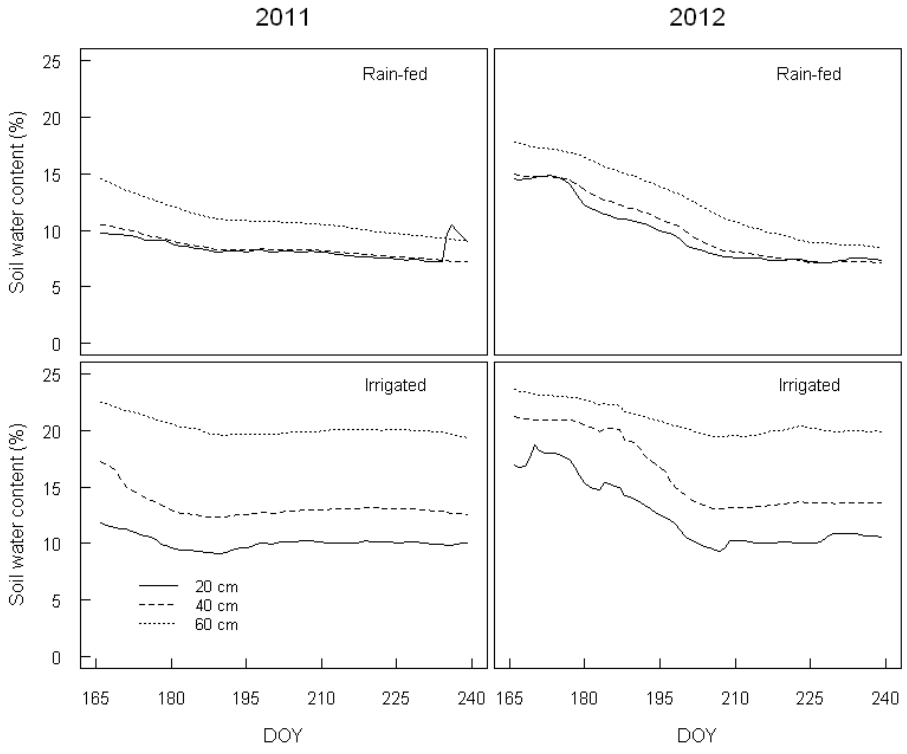

Figure 3. Soil water content at three depths (20, 40 and 60 cm) for rain-fed and irrigation treatments over the 2011 and 2012 growing seasons. DOY stands for Day of the Year (165 = 13th June).

Nonlin. Processes Geophys. Discuss., doi:10.5194/npg-2016-14, 2016
Manuscript under review for journal Nonlin. Processes Geophys.
Published: 23 February 2016

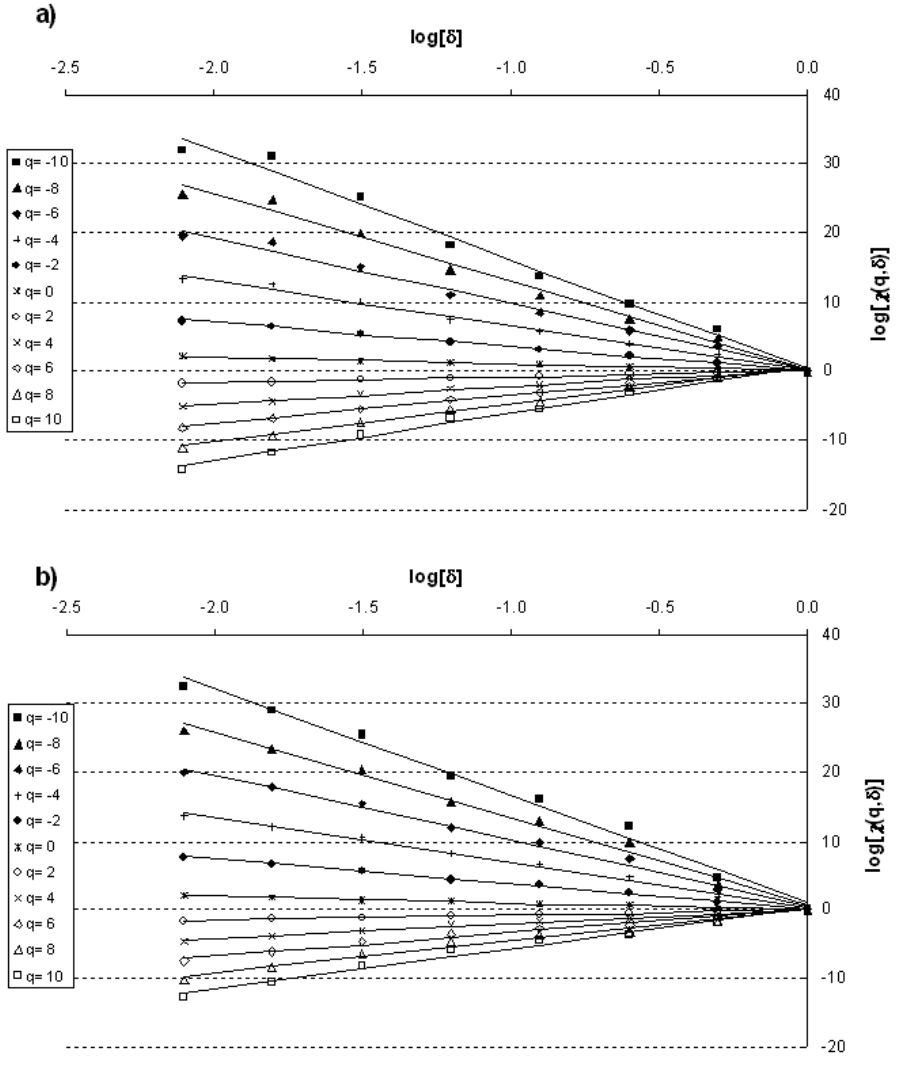

Figure 4. Selected plots of the natural logarithms of the partition function, $\chi(q,\delta)$, versus the time resolution, δ: a) rain-fed treatment at 20 cm depth in 2011; b) irrigated treatment at 20 cm depth in 2011.

Nonlin. Processes Geophys. Discuss., doi:10.5194/npg-2016-14, 2016
Manuscript under review for journal Nonlin. Processes Geophys.
Published: 23 February 2016

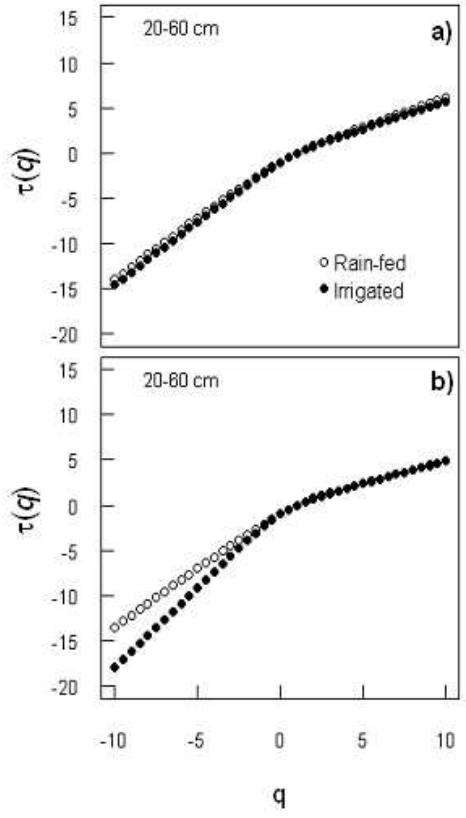

Figure 5. Mass exponents, $\tau(q)$, of soil water content averaged from 20 to 60 cm depth for rain-fed and irrigation treatments: a) 2011, b) 2012.

Nonlin. Processes Geophys. Discuss., doi:10.5194/npg-2016-14, 2016
Manuscript under review for journal Nonlin. Processes Geophys.
Published: 23 February 2016

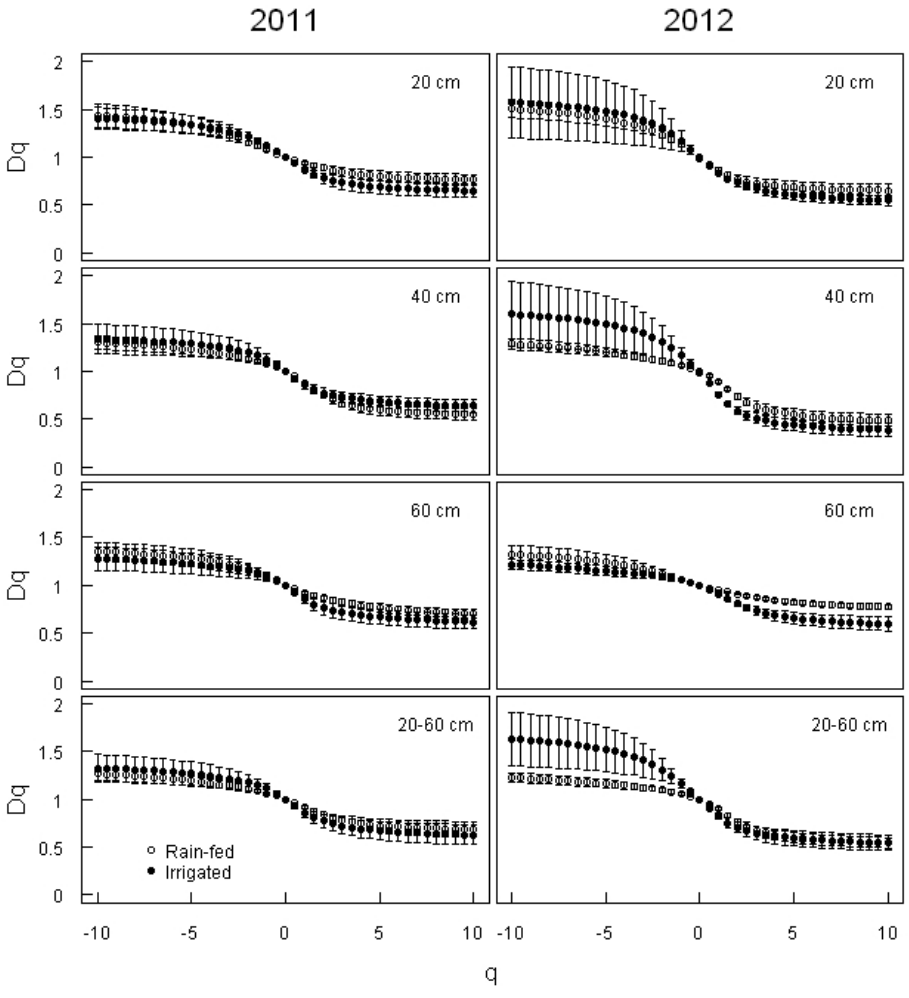

Figure 6. Generalized dimension, D_q, spectra ($-10 < q < 10$) of soil water content for rain-fed and irrigation treatments at the studied depths in 2011 and 2012. Bars indicate estimation errors.

Nonlin. Processes Geophys. Discuss., doi:10.5194/npg-2016-14, 2016
Manuscript under review for journal Nonlin. Processes Geophys.
Published: 23 February 2016

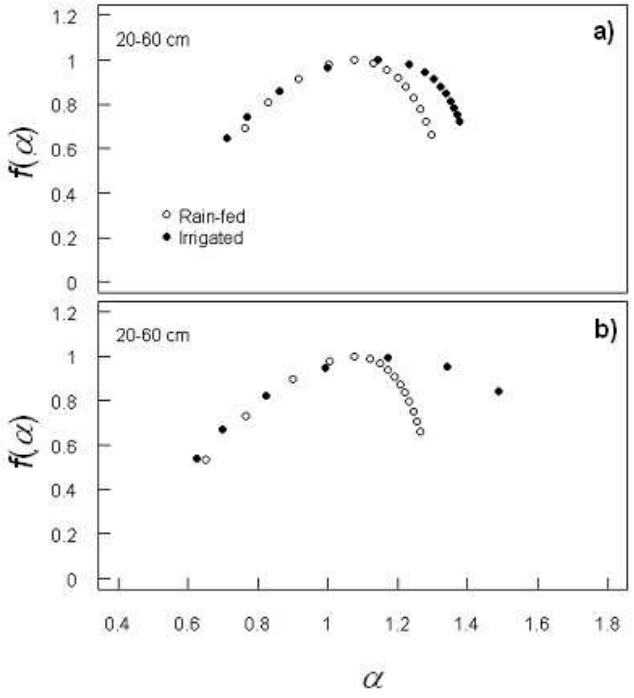

Figure 7. Singularity spectra for soil water content averaged from 20 to 60 cm depth for rain-fed and irrigation treatments: a) 2011, b) 2012.